Assessment of Edgewise Insulated Wire Bend Radius Impact on Dielectric Properties of Turn-to-Turn Insulation through Thermal Ageing

H. Naderiallaf, M. Degano, *Senior Member, IEEE*, and C. Gerada, *Senior Member, IEEE*

***Abstract*—This study aims to evaluate the impact of the bending radius of edgewise insulated wires on dielectric properties such as partial discharge inception voltage (PDIV), partial discharge extinction voltage (PDEV), dielectric dissipation factor (DDF), and insulation capacitance (IC) through thermal ageing. The tests are performed at room temperature (20°C) and atmospheric pressure (1013 mbar) on unaged and thermally aged polytetrafluoroethylene (PTFE)-wrapped pairs of edgewise insulated wires, models of the turn-to-turn insulation. The accelerated thermal ageing is carried out at 250°C (i.e., 50°C higher than thermal class) for two different ageing periods: 156 and 312 hours. To manufacture a coil, it is generally demanded to shape 90-degree bends out of edgewise enamelled winding wires. Therefore, the obtained experimental results are helpful for the coil manufacturers, providing a clue how the bending radius can impact the dielectric properties of turn-to-turn insulation and introducing an optimum radius which can present better insulation performance.**

***Index Terms*— Accelerated ageing, dielectric losses, dielectric measurement, electric machines, partial discharges, reliability.**

I. Introduction

RECTANGULAR wires are used to manufacture traction motor coils in electric vehicles (EVs) and hybrid electric vehicles (HEVs) to increase motor performance [1]. There are some advantages to employing rectangular insulated wires (e.g., edgewise ones) to manufacture the winding of electrical machines over random wound winding. The primary motivation is obtaining a high filling factor for reduced copper losses and higher power density [2]. Moreover, rectangular insulated wires usually have a larger insulation thickness than custom round wires, offering a higher partial discharge inception voltage (PDIV). In addition, controlling the turn-to-turn voltage is more manageable compared to random wound winding, as the location of the wires is more defined. However, there are some disadvantages to using rectangular insulated wires, such as skin effect losses, restricting the drive frequency [3], and more complex coil manufacturing (e.g., to the need for a forming machine with good accuracy, laser soldering and reinsulating the soldering points).

The turn-to-turn winding insulation is known as the most vulnerable insulation system in electrical machines playing a definitive role in the reliable machine's operation. Once the electric field corresponding to the turn-to-turn insulation exceeds the partial discharge (PD) inception field, PD activity is initiated, promoting insulation degradation, especially if the winding wires are insulated only with organic materials. In this case, PD can result in premature failure, reducing the life to a few days, if not hours [4], [5], [6]. Therefore, [7] advises that inverter-fed machines with Type I insulation (i.e., organic-only insulating materials) must be designed based on the PD-free criterion, i.e., the maximum peak voltage between two adjacent turns should remain lower than the minimum peak of PDIV [6]. Unfortunately, PDIV can reduce due to the inevitable insulation ageing (e.g., thermal ageing) and degenerating PD activity, thus, affecting the whole insulation system reliability [8].

The considered edgewise wire for this experimental study has Type I insulation (i.e., organic insulating materials), where PD is known as the end-of-life criterion [7]. It is very important to investigate if any damage or fraction for the insulation occurs during coil manufacturing through the bending of edgewise wires. As it is usually required to make 90-degree bends out of edgewise enamelled winding wires (Fig. 1), it will be necessary to know if the bending radius can affect the dielectric properties or if there is any optimum radius that can give better insulation performance.

Fig 1. A typical coil manufactured by edgewise insulated wires.

Thus, this paper discusses the relationship between PD activity and the bending radius of turn-to-turn winding insulation made from edgewise insulated wires subjected to

This paper was submitted for review in April 2023. This work was supported by the Clean Sky 2 Joint Undertaking through the European Union's Horizon 2020 Research and Innovation Programme under Grant 807081. *(Corresponding author: Hadi Naderiallaf).*

Hadi Naderiallaf, Michele Degano, and Chris Gerada are with the Power Electronics and Machines and Control (PEMC) Research Group, the University of Nottingham, Nottingham, U.K. (e-mail: Hadi.Naderiallaf@nottingham.ac.uk; Michele.Degano@nottingham.ac.uk; Chris.Gerada@nottingham.ac.uk).

thermal ageing. The electric field in the turn-to-turn insulation systems follows a capacitive distribution. Therefore, the dielectric dissipation factor (DDF) and insulation capacitance (IC) measurements are also performed on turn-to-turn samples (both straight and bent specimens), investigating their correlations with PDIV values.

The structure of this paper is as follows. Section II introduces the test samples, measurement conditions, the approach used to measure PDIV and PDEV, and the method to measure the DDF and IC. In Section III-A, the measured PDIV and PDEV as a function of bend radius for different levels of thermally aged specimens are presented. Section III-B explores the correlation between PDIV and the insulation thickness as a function of thermal ageing for different bend radii. Section III-C examines the influence of bend radius on the DDF and IC at different ageing levels. Section III-D proposes an equivalent circuit for the bent turn-to-turn samples. Section III-E shows the dispersion level of measured PDIV and PD charge amplitude vs thermal ageing time for different bend radii. Section III-F discusses the measured PD charge amplitude, PD repetition rate, and the severity index under PDIV as a function of bend radius at different ageing levels. Section III-G presents the measured DDF tip-up values for straight and bent samples for fresh and thermally aged samples. In Section III-H, the derived correlation between the measured PDIV and the dissipation parameters for turn-to-turn samples with different bend radii is shown. Section VI summarizes the main results of the work.

II. Methodology

A. Test Samples Characteristics and Manufacture

Fig. 2 displays the test samples preparation procedure. PD, DDF and capacitance measurements are carried out on unaged and thermally aged polytetrafluoroethylene (PTFE)-wrapped pairs of edgewise insulated wires, mirroring the turn-to-turn insulation system (Fig. 3b) [8]. The test samples are categorized into two main groups: 1) straight (STR.) and 2) bent turn-to-turn specimens. Three different bend radii: 8.5, 6.5 and 3.5 mm, are considered to make 90-degree bends out of edgewise enamelled winding wires (Fig. 3). The bend radius of 3.5 mm is often the smallest bend radius for edgewise insulated wires used by the coil manufacturers. The two additional radii, both larger than 3.5 mm, are included with the sole purpose of establishing a trend for various parameters derived from at least three different bend radii. It is noteworthy to mention that the samples are bent using the same procedure employed in manufacturing an actual coil with edgewise wire. Furthermore, PTFE is employed to hold the two wires securely and near each other. Based on this, it is presumed that real coils also possess similar vulnerable points at the extreme sections, where PD activity may occur due to the bending and separation of the wires. This assumption is made because the bending technique and coil manufacturing process are identical to those used for the sample preparation.

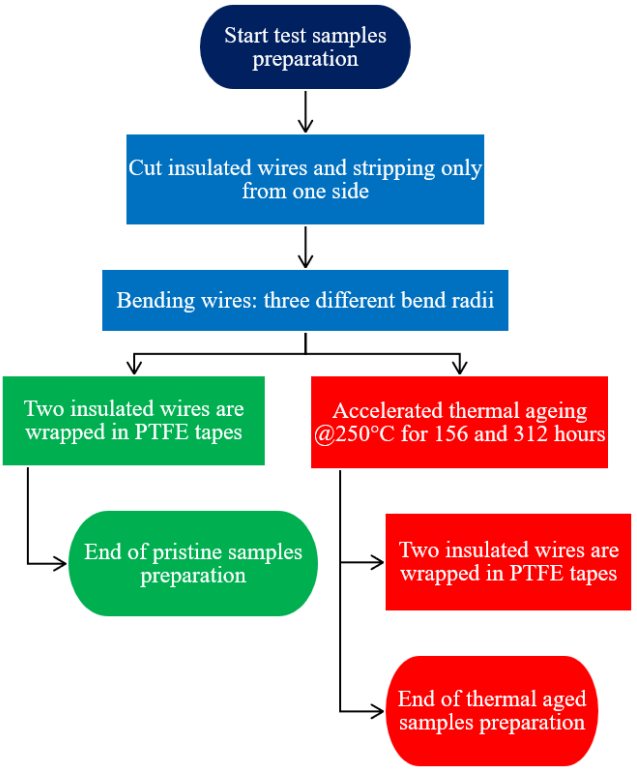

Fig. 2. A flowchart to visualize the test samples preparation process.

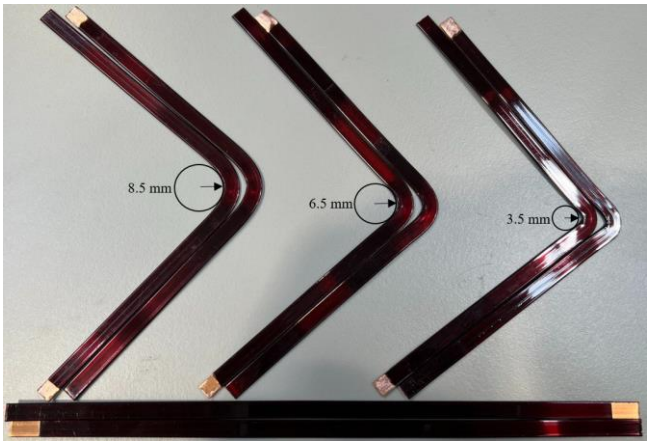

(a)

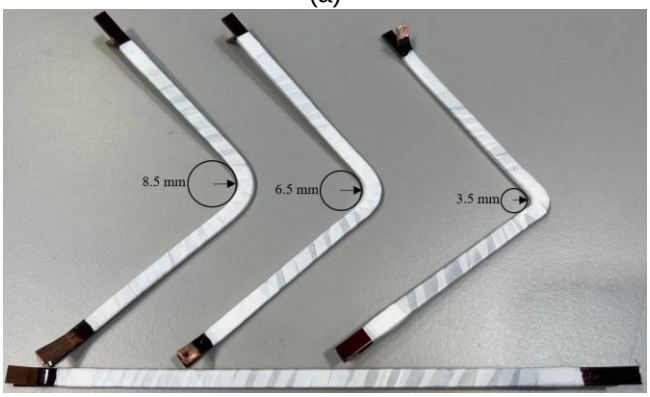

(b)

Fig. 3. Straight and bent edgewise insulated wires (a) before and (b) after wrapping by PTFE.

Fig. 4 depicts the wire cross-section, indicating bare wire dimensions and the insulation thickness. The dimensions are the mean value obtained from 32 wires by differencing the dimension values before and after stripping wires using a micrometre with an accuracy of 1 µm [9]. The wire is stripped using a laser wire stripping machine, ensuring only the insulation is removed and not any portion of copper. The thermal class of the wires enamel is 200°C, composed of a polyester-imide/polyester basecoat and a polyamide-imide overcoat. The length of each wire to assemble the test samples is 22 cm.

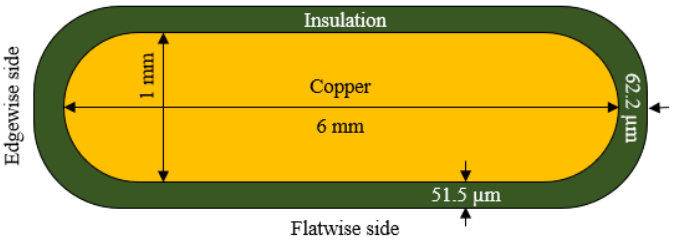

Fig. 4. Edgewise insulated wire cross-section dimensions.

The accelerated thermal ageing process is performed at 250°C (i.e., 50°C higher than the thermal class) for two different ageing periods: 156 and 312 hours. In this study, the "ten-degree" approach is employed to provide a rough estimation of insulation deterioration. According to this rule, the lifespan of insulation is divided by two for every 10°C increase in temperature above the thermal index (TI) [10]. For example, if the expected longevity of an insulation system at TI (e.g., TI = 200°C for the insulation under investigation) is 20,000 hours, exceeding the temperature by 50°C above TI (i.e., 250°C) dramatically reduces the lifetime to approximately 625 hours. To investigate the impact of higher temperatures on insulation performance over an extended period, the accelerated thermal ageing is carried out at 250°C for 156 hours and 312 hours, corresponding to approximately 25% and 50% of the overall insulation lifetime, respectively. Consequently, the results obtained from this experimental study pertain to the turn-to-turn winding insulation and its behaviour up to 50% of the insulation's total lifespan. The decision to limit the ageing duration to the timeframe of 312 h is also driven by the objective of preventing excessive brittleness of the insulation, which could lead to the formation of cracks during the sample preparation process when wrapping the thermally aged pairs with PTFE. In other words, the insulation's brittleness at 250°C and after 312 h reached a manageable level, making it possible to wrap the wires with PTFE by hand without causing cracks in the insulation. Thus, the chosen approach allows for a focused investigation of the impact of thermal ageing without the interference of additional factors arising from excessive brittleness or cracks. Fig. 5 shows the insulated wires in the oven before starting the accelerated thermal ageing process. After finishing each thermal ageing period, the two portions of insulated wire (i.e., straight or bent wires) are wrapped in PTFE tapes. Therefore, the test samples are categorized into three main groups from the ageing condition point of view: 1) pristine samples and thermally aged specimens for 2) 156 h and 3) 312 h. For each ageing condition, four sets (i.e., straight, 8.5, 6.5 and 3.5 mm) of ten (i.e., five samples for PD tests and five specimens for DDF and capacitance tests) PTFE-wrapped pairs each are manufactured out of the edgewise winding wires.

Fig. 5. Edgewise insulated wires inside the oven before the accelerated thermal ageing process.

B. Common Measurement Conditions: PD and (DDF, IC) Tests

All the measurements are performed at room temperature (20°C), atmospheric pressure (1013 mbar) and relative humidity (30±5%). The environmental conditions are controlled by a fully controlled Memmert pass-through oven. The specimens are located inside the oven, with one wire of the turn-to-turn samples connected to the AC power supply and one to the ground (Fig. 6). All the tests for each combination of the turn-to-turn samples construction (i.e., straight and bent: three different radii) and ageing conditions (i.e., pristine, and thermally aged: 156 and 312 h) are performed using five specimens to collect the set of data for each case study. It is important to emphasize that PD is a destructive phenomenon, especially when it occurs in organic insulation, such as polyamide-imide. In this context, PD is regarded as a crucial insulation end-of-life criterion [7]. Upon conducting repeated tests on the same specimen, it is observed that the PDIV values decreased. Therefore, each sample is tested only once to prevent the possible impact of previous measurements (e.g., PDIV drop caused by previous discharge activities) [11].

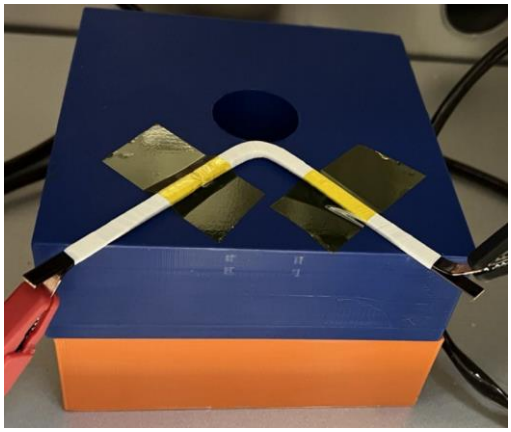

Fig. 6. A typical test specimen under test.

C. AC PDIV and PDEV Testing

PD tests are performed under a sinusoidal waveform excitation at a power supply frequency of 50 Hz. It is noteworthy to highlight that the IEC [7] allows PDIV testing using either sinusoidal or impulsive voltages to be used for the turn-to-turn insulation qualification of inverter-fed motors. The PDIV values tend to be lower when subjected to sinusoidal excitations compared to that of PWM with rise times shorter than 1 µs [12]. Even when PDIV is measured using a 50 Hz sinusoidal power source, the results remain consistent, offering a slightly more cautious evaluation of PDIV for turn-to-turn insulation under the influence of a 2-level inverter or surge generator, as discussed in [13], [14], [15]. Additionally, comparative PDIV tests conducted on twisted pairs as described in [16] revealed that AC excitations result in the lowest PDIV values compared to PWM. Based on these findings, a conservative approach is adopted in this investigation, where PDIV measurements are carried out under AC 50 Hz excitations. Apart from that, it should be noted that the primary objective of this paper, however, is to analyze and evaluate how the bending radius affects PDIV. This evaluation can be conducted using any waveform, but it is crucial to maintain a consistent waveform throughout the study.

The AC source is GPT-9802, manufactured by GW Instek. The peak voltage is raised in steps of 10 V every 30 s, [8], [17], and monitored through a Teledyne LeCroy WaveSurfer 510 oscilloscope (1 GHz bandwidth, 10 GS/s sampling rate) using a CT4079-NA differential probe (50 MHz bandwidth, 2000:1 voltage ratio, 50 Ω impendence). The peak value of the voltage is recorded as PDIV as soon as PD activity is initiated. After measuring PDIV, the peak voltage is reduced in steps of 10 V peak each minute [8], [17]. When PD activity is extinct, the peak voltage is recorded as PDEV.

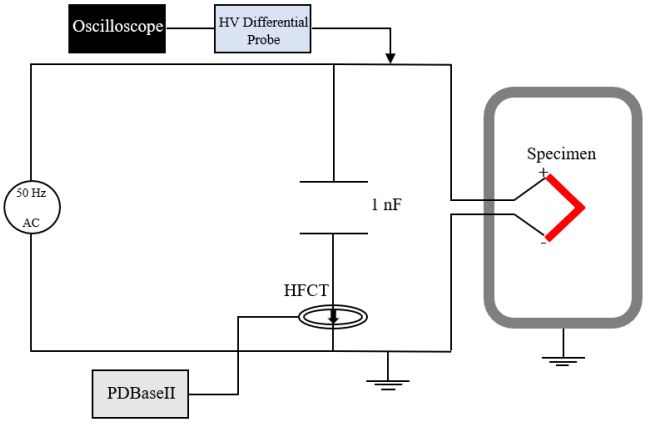

Fig. 7. Circuit and connections layout for PD test setup.

PD detection is carried out with a conventional indirect circuit schematized in Fig. 7. A PD-free 1 nF coupling capacitor is used in parallel with the test specimen to amplify the PD signal, improving the detection sensitivity. The PD sensor to acquire the PD pulses is a ferrite-core high-frequency current transformer (HFCT) with 1-60 MHz bandwidth manufactured by Techimp HQ. The discharge current signal is recorded and processed through IEC 60270-compliant instrumentation (i.e., Techimp PDBaseII detector). The PDBaseII features a range of frequency acquisition from 16 KHz to 48 MHz, a sampling rate of 200 MSa/s, and delivers the PD pulse waveform [18]. The PD calibration is accomplished for each test specimen separately using PDCAL PLUS manufactured by Techimp HQ, which can produce up to 800 pC pulses. It is worthwhile to note that the PD BaseII is equipped with specialized IEC software that allows for the conversion of PD charge amplitude values from millivolts (mV) to pico coulombs (pC) in the pattern after calibration. This functionality ensures that the PD magnitude is measured within a specific frequency bandwidth, consistent with the range defined by IEC 60270, which spans from 115 KHz to 440 KHz.

D. DDF and IC Measurements

The DDF and IC tip-up testing (i.e., $\Delta\tan\delta$ and ΔC) of each turn-to-turn sample is accomplished at 50 Hz using a sinusoidal voltage waveform by adopting a Megger Delta4000 [19]. The peak of applied sinusoidal voltage at 50 Hz is increased from zero to 1.27 kV with a step of 39 V. The choice of selecting 1.27 kV as the voltage level is driven by the intention to use a value well above the PDIV. This higher voltage level allows for the clear visualization of two distinct regions in the dissipation factor curve compared to the applied voltage (see later Fig. 18). The first region in the curve exhibits an almost flat dissipation factor versus the applied voltage, indicating the presence of conduction and polarization losses. The second region, on the other hand, displays a rising trend of the dissipation factor as the applied voltage increases, signifying the occurrence of ionization losses. As for the choice of 39 V, it is made to ensure that there are sufficient data points after ionization has taken place. This decision ensures that the trend in the ionization region can be observed and analysed with clarity. Five specimens are tested for each case study. Also, each sample is measured once to avoid the influence of the previous measurement. Finally, the average value is reported.

III. Experimental Results and Discussions

The PD measurement results are depicted and plotted as a function of thermal ageing time using boxplots to provide a clear visual insight. Each box summarizes a data set by showing the median value, q_2 (central line in the box), the 25th, q_1, and 75th, q_3, percentiles (the edge of the box), the data range (using whiskers at q_2-1.5×(q_3-q_1) and q_2+1.5×(q_3-q_1)). The small square symbol inside each box demonstrates the mean value [20], [17]. The connection line of the boxes relates to the mean value, illustrating the PD quantities (i.e., PDIV, PDEV, PD charge amplitude and repetition rate) trend as a function of bend radius for each thermal ageing period.

A. PDIV and PDEV Analysis

Fig. 8 shows the measured peak value of PDIV as a function of thermal ageing time for straight and bent samples. Table I denotes the mean values of PDIV corresponding to Fig. 8.

According to Fig. 8 and Table I, PDIV diminishes as a function of thermal ageing time for all the samples, regardless of the bend radius. Considering the fresh specimens and each thermal ageing period (i.e., 156 and 312 h), interestingly, bent turn-to-turn samples deliver a higher PDIV than the straight ones. It means the bending process with a bend radius down to 3.5 mm does not lead to fraction/cracking in the insulation. Although the bent samples with a larger bend radius provide a higher PDIV before starting the ageing process (i.e., for the pristine specimens), the results after thermal ageing show that the bent samples with the bend radius of 6.5 mm provide the highest PDIV values, suggesting an optimum bend radius for the edgewise insulated wire.

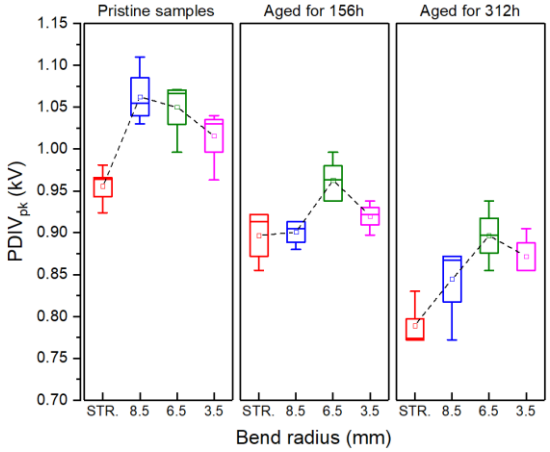

Fig. 8. PDIV trend consequent to thermal ageing under AC (50 Hz) excitation for straight (STR.) specimens vs bent ones with three different radii.

TABLE I
THE MEAN VALUES OF PDIV RELEVANT TO FIG. 8

Bend radius (mm)	Pristine samples	Aged for 156 h	Aged for 312 h
	PDIV$_{pk}$ (kV)		
Straight	0.956	0.897	0.789
8.5	1.06	0.901	0.845
6.5	1.05	0.963	0.897
3.5	1.02	0.92	0.872

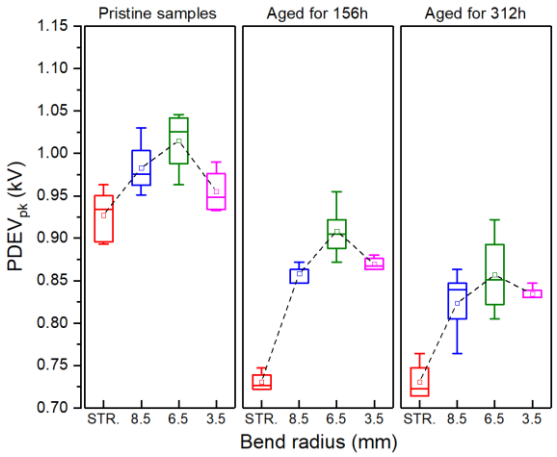

Fig. 9. PDEV trend consequent to thermal ageing under AC (50 Hz) excitation for straight (STR.) specimens vs bent ones with three different radii.

TABLE II
THE MEAN VALUES OF PDEV RELEVANT TO FIG. 9

Bend radius (mm)	Pristine samples	Aged for 156 h	Aged for 312 h
	PDEV$_{pk}$ (kV)		
Straight	0.927	0.731	0.731
8.5	0.983	0.858	0.824
6.5	1.02	0.908	0.857
3.5	0.955	0.87	0.834

Fig. 9 displays the measured peak value of PDEV as a function of thermal ageing time for straight and bent samples. Table II reports the mean values of PDEV corresponding to Fig. 9. Fig. 9 and Table II indicate that the same as PDIV, the bent turn-to-turn samples deliver higher PDEV values than the straight samples. The bent specimens with a bend radius of 6.5 mm provide the highest PDEV both before and after the thermal ageing process.

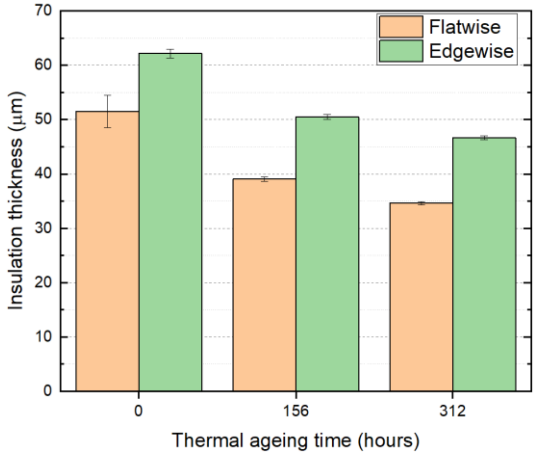

Fig. 10. Insulation thickness vs thermal ageing time.

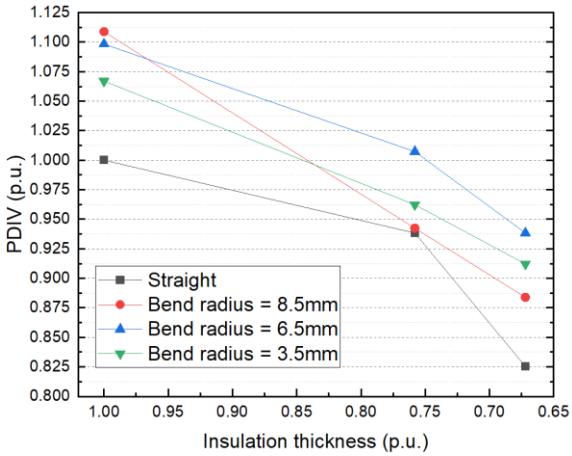

Fig. 11. Correlations between PDIV and insulation thickness, normalized to unaged straight mean.

B. Correlation between PDIV and Insulation Thickness Shrinking

The reason for the PDIV mitigation consequent to thermal ageing is most likely due to the insulation thickness reduction caused by the polyamide-imide vaporization resulting from the thermal ageing at 250°C. Fig. 10 displays the insulation thickness shrinking of the edgewise insulated wire as a function

of thermal ageing time for both flatwise and edgewise directions. Each bar chart reports the mean value of 32 measured samples. The insulation thickness is reduced by 16.9 µm and 15.47 µm for flatwise and edgewise sides, respectively, after 312 h of thermal ageing at 250°C. Fig. 11 illustrates the correlations between PDIV drop and insulation thickness shrinking (i.e., flatwise side) due to thermal ageing. The values are normalized to unaged straight mean.

C. DDF and IC Analysis

The reason for a slightly higher PDIV for the bent specimens than the straight ones can be ascribed to the bent samples' higher conducting losses and lower capacitance [21]. Figs. 12a and 12b represent the variation of starting value or absolute DDF value, $\tan\delta_0$, indexing the conducting and polarization losses [22], and capacitance, C_0, at a low voltage (39 V_{rms}) as a function of bend radius and thermal ageing time, respectively, normalized to unaged straight mean.

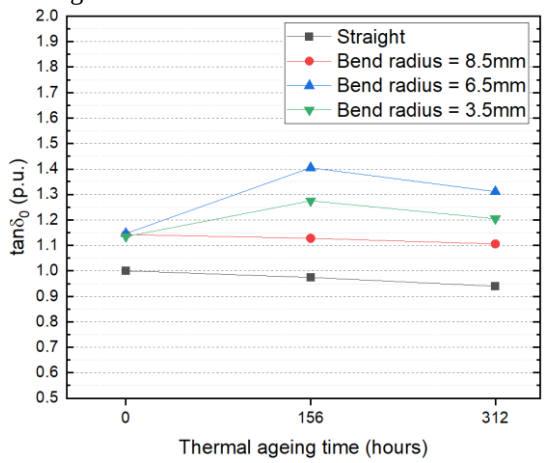

(a)

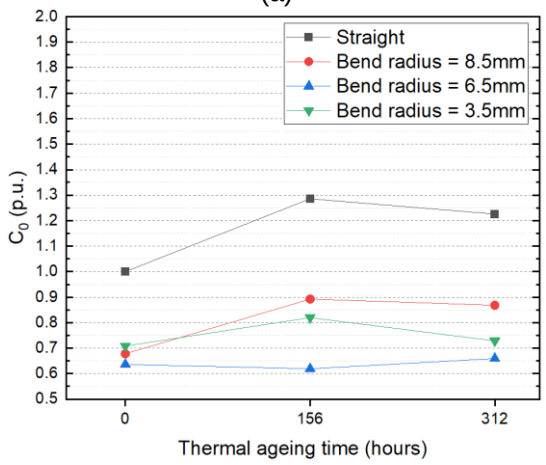

(b)

Fig. 12. The variation of (a) starting value or absolute DDF, $\tan\delta_0$, and (b) capacitance, C_0 at a low voltage (39 V_{rms}) as a function of bend radius and thermal ageing time, normalized to unaged straight mean.

Fig. 12 demonstrates that the bent turn-to-turn samples have higher conducting and polarization losses (i.e., $\tan\delta_0$) and lower capacitance (C_0) regardless of the ageing condition of the specimens. In addition, Fig. 12 shows that the bent samples with a bend radius of 6.5 mm, which deliver the largest PDIV and PDEV after thermal ageing (Figs. 8 and 9), features also the highest and lowest $\tan\delta_0$ and C_0, respectively, after starting the thermal ageing process.

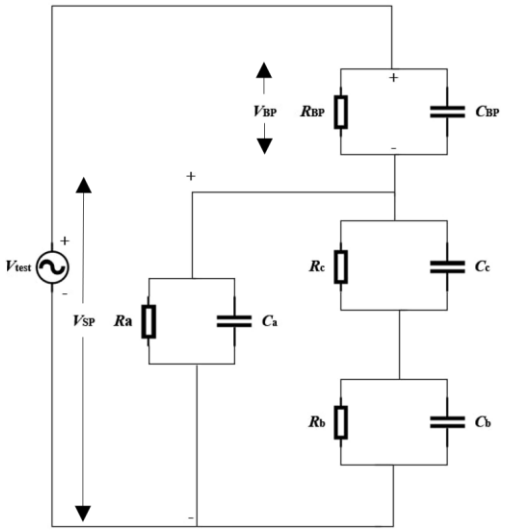

Fig. 13. Equivalent charging circuit for the bent samples.

D. Equivalent Charging Circuit for the Bent Turn-to-Turn Samples

Fig. 13 illustrates the equivalent circuit of the bent samples to clarify the contribution of the bending point resistance and capacitance to delivering a higher PDIV. It is worthwhile to recall that dielectric materials can be represented using either parallel or series equivalent circuits, and both approaches are considered acceptable. However, for this specific case, the series configuration is chosen, linking the straight part to the bending point. The reason behind this choice is that the series configuration allows for easier management and provides a clear and distinctive view of both the straight part and the bending point of the bent turn-to-turn wire insulation. In Fig. 13, R_{BP} and C_{BP} are bending point resistance and capacitance, V_{BP} is the voltage drop across the bending point, V_{SP} is the voltage across the straight part, R_c and C_c are resistance and capacitance of defect where discharges occur, R_b and C_b are resistance and capacitance of the dielectric in series with the defect, and R_a, C_a are the remaining resistance and capacitance of the test sample. R_{BP} and C_{BP} have a reverse and direct relationship with the insulation cross-section at the bending point, A, respectively.

$$R_{BP} \propto \frac{1}{A} \quad (1)$$

$$C_{BP} \propto A \quad (2)$$

According to the equivalent circuit introduced in Fig. 13, the bending point impedance, Z_{BP}, is equal to:

$$|Z_{BP}| = \frac{1}{\sqrt{(\frac{1}{R_{BP}})^2 + (\omega \cdot C_{BP})^2}} \quad (3)$$

When the edgewise insulated wire is bent, and if the insulation is still healthy at the bending point (i.e., free from any fraction/cracking), the insulation cross-section, A, reduces due to squeezing at the bending site, leading to an increase and decrease of R_{BP} and C_{BP}, respectively. Therefore, the bending point impedance, Z_{BP}, increases, resulting in a higher voltage drop across the bending point, V_{BP}. Eventually, a higher test voltage, V_{test}, thus PDIV, will be needed to incept PD. Considering (3), it can be speculated that the PDIV difference between straight and bent sample can be negligible if the supply frequency increases due to the reduction of Z_{BP}.

E. Dispersion of PDIV and PD Charge Amplitude under PDIV

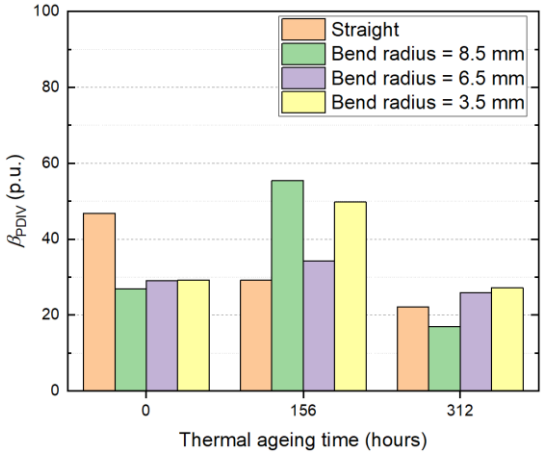

Fig. 14. PDIV dispersion level as a function of thermal ageing time.

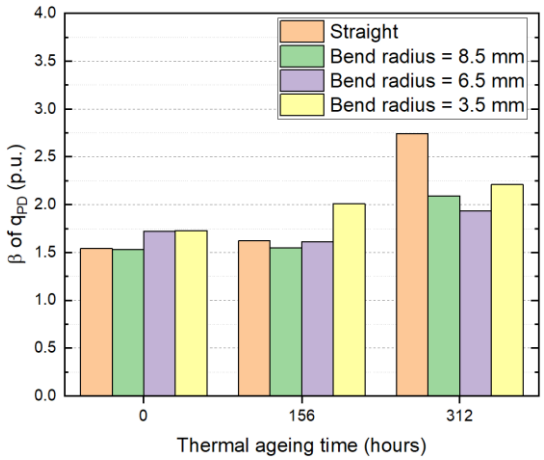

Fig. 15. PD charge amplitude dispersion level as a function of thermal ageing time under PDIV.

Figs. 14 and 15 quantify the dispersion level of the peak value of PDIV and PD charge amplitude, q_{PD}, under PDIV consequent to thermal ageing time for straight and bent samples, relying on the shape/slope parameter of the 2-parameter Weibull distribution (i.e., β). Fig. 14 shows that β_{PDIV} steadily reduces or PDIV dispersion increases for the straight samples as a function of the thermal ageing period. For the bent turn-to-turn specimens, while it promotes after 156 hours of ageing, the opposite occurs for a longer thermal ageing period. β_{PDIV} diminishes/PDIV dispersion increases for all the samples after 312 hours of thermal ageing time, manifesting a diagnostic marker for the thermal ageing of polyamide-imide.

Regarding the PD charge amplitude, at least 2000 PD pulses are acquired to perform the Weibull analysis automatically using the PD BaseII software. Fig. 15 demonstrates that the β of q_{PD} increases or PD charge amplitude dispersion decreases as a function of the thermal ageing period, manifesting another ageing indicator for polyamide-imide. In addition, Fig. 15 shows that before 312 h of thermal ageing, the contribution of surface PD is more than the internal PD activity (i.e., $\beta < 2$). However, the opposite occurs after 312 h (i.e., $2 < \beta < 4.8$) when more contribution of internal PD in the voids caused by the thermal ageing process would be plausible [23]. After 312 h, the β of q_{PD} for $r_{\mathrm{Bend}} = 6.5\,mm$ is still lower than two, verifying the less possibility of void creation in the insulation consequent to the thermal ageing compared with other bend radii.

F. PD Charge Amplitude, Repetition Rate, and Severity Analysis under PDIV

Figs. 16a and 16b report the trend of $Q_{\mathrm{max,95\%}}$ (the 95$^{\mathrm{th}}$ percentile of PD charge amplitude distribution) in pC and PD repetition rate, N_{w}, in pulse per period (ppp), respectively, under PDIV over the thermal ageing period, comparing the straight samples vs the bent ones with different bend radii.

In general, both $Q_{\mathrm{max,95\%}}$ and PD repetition rate are decreased as a function of thermal ageing time which can be attributed to lower PDIV for the thermally aged samples (Fig. 8). After 312 hours, $Q_{\mathrm{max,95\%}}$ is comparable for different bend radii (Fig. 16a), while PD repetition rate is higher for smaller bend radii (Fig. 16b).

To better describe and compare the straight samples vs the bent ones based on harmfulness or damage associated with PD activity under PDIV through thermal ageing time, a diagnostic dimensionless quantity known as the PD severity index (Idx) can be introduced such as one devised in [24], [25], [26], [27], by simply multiplying $Q_{\mathrm{max,95\%}}$ and N_{w} values as (4):

$$Idx = Q_{\mathrm{max,95\%}} \cdot N_{\mathrm{w}} \tag{4}$$

Fig. 17 reports the Idx trend during the thermal ageing time, comparing the straight edgewise insulated wires against the bent ones with different radii, using (4) based on the mean values reported in Fig. 16. Idx shows the lowest and highest value for $r_{\mathrm{Bend}} = 6.5\,mm$ and $8.5\,mm$, respectively, for unaged turn-to-turn samples. However, after thermal ageing, Idx is minimum for the straight turn-to-turn specimens while manifesting a higher value for a smaller bend radius. As a result, the harmfulness or damage associated with PD activity is higher for the bent turn-to-turn samples than the straight ones consequent to thermal ageing. In addition, there is a reduction trend for Idx with respect to the thermal ageing time, which can

be ascribed to lower PDIV for the thermally aged specimens (Fig. 8).

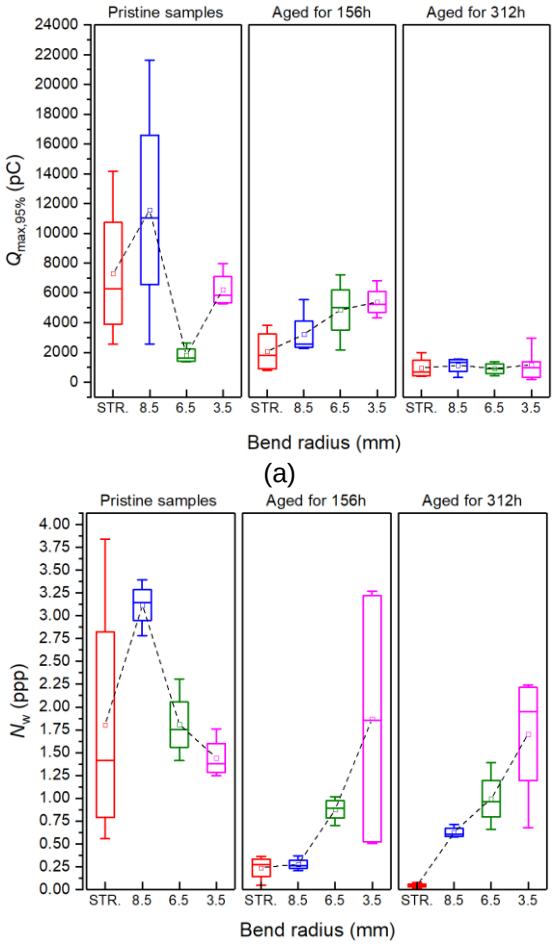

Fig. 16. $Q_{\max,95\%}$ and N_w trend of PD detected under PDIV during the thermal ageing time for straight (STR.) specimens vs bent ones with three different radii.

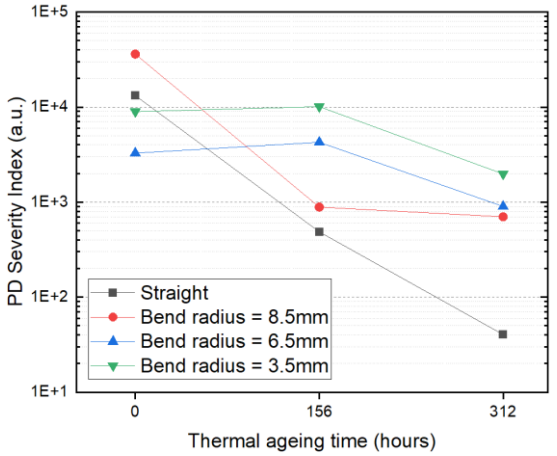

Fig. 17. PD Severity Index under PDIV (straight specimens vs bent ones) through thermal ageing time.

G. DDF TIP-UP Testing (Fresh vs Thermally Aged four 312 h)

Fig. 18 summarizes the measurement results of tanδ tip-up using a sinusoidal waveform at 50 Hz, comparing the straight with bent turn-to-turn samples and the pristine specimens vs the thermally aged ones for 312 h. Fig. 18 shows that the thermally aged straight turn-to-turn samples give the highest DDF after ionization (i.e., when tanδ steeply starts to rise). Considering only the unaged specimens or the thermally aged ones, the straight samples deliver the highest ionization losses since the more electric field is concentrated across the defect once ionization starts due to the absence of R_{BP} (Fig. 13). For the bent turn-to-turn samples, tanδ starts to increase due to ionization at a higher voltage level than the straight specimens, verifying the obtained results via PD tests (i.e., $PDIV_{STR.} < PDIV_{Bent}$).

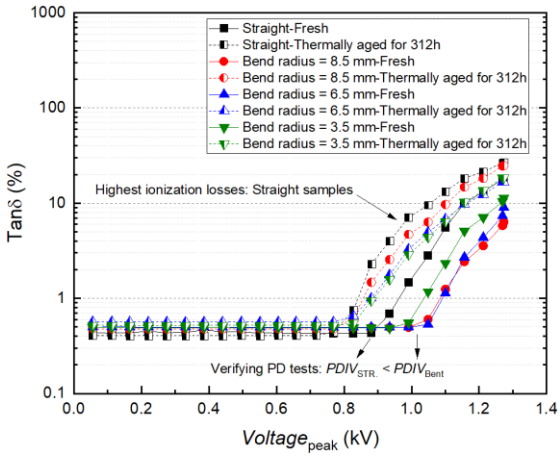

Fig. 18. The variation of DDF as a function of test voltage measured at 50 Hz for the straight turn-to-turn samples with the bent ones and the unaged specimens vs the thermally aged ones for 312 h.

H. Correlation Between PDIV and Dissipation Parameters

Figs. 19a and 19b display the correlation plots between the PDIV and the dissipation parameters of $\Delta\tan\delta_{H\text{-}L}$ and $\Delta C_{H\text{-}L}$, respectively, consequent to the thermal ageing. The value of $\Delta\tan\delta_{H\text{-}L}$ is the difference between the DDF corresponding to the highest applied voltage (i.e., 900 V_{rms}) and the DDF measured at the lowest applied voltage (i.e., 39 V_{rms}). A similar definition stands for $\Delta C_{H\text{-}L}$, introducing the capacitance difference between the lowest and highest applied voltages. The values in Fig. 19 are normalized to unaged straight mean.

A higher value of $\Delta\tan\delta_{H\text{-}L}$ and $\Delta C_{H\text{-}L}$ can be a marker for enhancing the number and size of voids or the formation of delamination in the insulating system [21], [22]. Overall, Fig. 19 denotes that the bent turn-to-turn specimens with a radius of 6.5 mm deliver a lower $\Delta\tan\delta_{H\text{-}L}$ and $\Delta C_{H\text{-}L}$, implying less possibility for voids or delamination in the insulation system. In addition, Fig. 19 demonstrates that higher dissipation parameters (i.e., $\Delta\tan\delta_{H\text{-}L}$ and $\Delta C_{H\text{-}L}$) reflect lower PDIV values, indicating a good correlation.

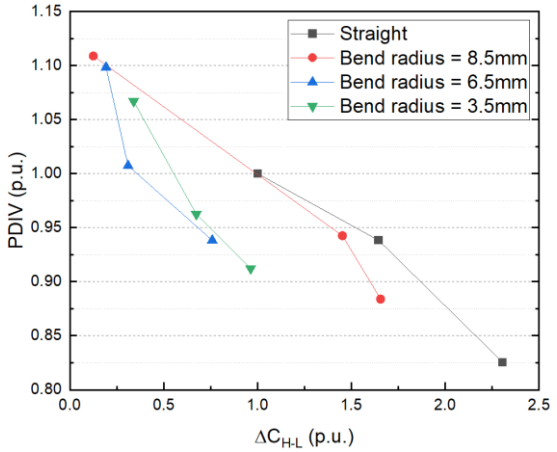

(a)

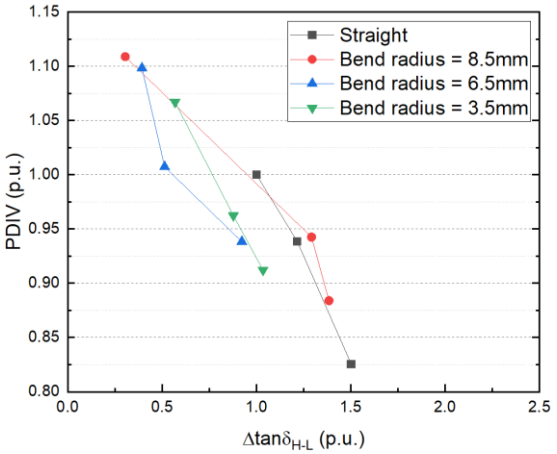

(b)

Fig. 19. The correlation plots between the PDIV and the dissipation parameters of (a) $\Delta\tan\delta_{H\text{-}L}$ and (b) $\Delta C_{H\text{-}L}$, normalized to unaged straight mean.

VI. Conclusion

This contribution shows that bending edgewise insulated wires carried out during coil manufacturing can result in higher PDIV and PDEV than the straight turn-to-turn insulation. It is demonstrated that among the considered bend radii, $r_{\text{Bend}} = 6.5\ mm$ gives the highest PDIV and PDEV after thermal ageing of the turn-to-turn samples. Moreover, higher conducting and polarization losses (i.e., $\tan\delta_0$) and a lower turn-to-turn capacitance belong to the bent specimens, especially $r_{\text{Bend}} = 6.5\ mm$, after thermal ageing. It means that bending wires results in PDIV rise in the cost of increasing losses which should be considered during coil manufacturing. Regarding the capacitance reduction due to bending, it should be mentioned that it can be favoured for inverter-fed motors using steep-fronted square waveform excitations. It is due to this fact that a lower capacitance of the coil helps the rise time to be shorter, closer to the one designed for the inverter's waveform, while the opposite limits the rise time of the excitation.

It is substantiated that PDIV drop after thermal ageing is due to the insulation thickness shrinking. The severity index calculations show that the harmfulness or damage associated with PD activity can be higher for the bent turn-to-turn samples with a smaller bend radius after thermal ageing. In addition, two ageing indicators are introduced for the edgewise insulated wire (i.e., polyamide-imide): β_{PDIV} and β of q_{PD}. The former and latter decreases and increases, respectively, consequent to thermal ageing after 312 h. Finally, good correlations between PDIV and dissipation parameters (i.e., $\Delta\tan\delta_{H\text{-}L}$ and $\Delta C_{H\text{-}L}$) are introduced for edgewise insulated wires. To create a coil, edgewise enamelled winding wires must typically be bent at 90 degrees. The acquired experimental results are useful for coil makers because they show how the bending radius can affect the dielectric characteristics of turn-to-turn insulation and introduce an ideal radius that can show superior insulation performance.

References

[1] T. Wakimoto, H. Kojima and N. Hayakawa, "Measurement and evaluation of partial discharge inception voltage for enameled rectangular wires under AC voltage," *IEEE Trans. Dielectr. Electr. Insul.*, vol. 23, no. 6, pp. 3566-3574, Dec. 2016.

[2] T. Okada, H. Matsumori, T. Kosaka and N. Matsui, "Hybrid excitation flux switching motor with permanent magnet placed at middle of field coil slots and high filling factor windings," *CES Transactions on Electrical Machines and Systems*, vol. 3, no. 3, pp. 248-258, Sept. 2019.

[3] Y. Zhao, D. Li, T. Pei and R. Qu, "Overview of the rectangular wire windings AC electrical machine," *CES Transactions on Electrical Machines and Systems*, vol. 3, no. 2, pp. 160-169, June 2019.

[4] D. Fabiani and G. C. Montanari, "The effect of voltage distortion on ageing acceleration of insulation systems under partial discharge activity," *IEEE Electrical Insulation Magazine*, vol. 17, no. 3, pp. 24-33, May-June 2001.

[5] A. Cavallini, D. Fabiani and G. C. Montanari, "Power electronics and electrical insulation systems - part 2: life modeling for insulation design," *IEEE Electrical Insulation Magazine*, vol. 26, no. 4, pp. 33-39, July-Aug. 2010.

[6] M. Galea, P. Giangrande, V. Madonna and G. Buticchi, "Reliability-oriented design of electrical machines: the design process for machines' insulation systems must evolve," *IEEE Industrial Electronics Magazine*, vol. 14, no. 1, pp. 20-28, Mar. 2020.

[7] IEC Std. 60034-18-41, *Rotating electrical machines - part 18-41: partial discharge free electrical insulation systems (Type I) used in rotating electrical machines fed from voltage converters - qualification and quality control tests.* 2019.

[8] H. Naderiallaf, P. Giangrande and M. Galea, "A contribution to thermal ageing assessment of Glass fibre insulated wire based on partial discharges activity," *IEEE Access*, vol. 10, pp. 41186-41200, 2022.

[9] D. R. Meyer, A. Cavallini, L. Lusuardi, D. Barater, G. Pietrini, and A. Soldati, "Influence of impulse voltage repetition frequency on RPDIV in partial vacuum," *IEEE Trans. Dielectr. Electr. Insul.*, vol. 25, no. 3, pp. 873-882, 2018.

[10] IEEE Std 117-2015 (Revision of IEEE Std 117-1974), *IEEE Standard Test Procedure for Thermal Evaluation of Systems of Insulating Materials for Random-Wound AC Electric Machinery*, vol., no., pp. 1-34, May 6, 2016.

[11] M. Goldman, A. Goldman and J. Gatellet, "Physical and chemical aspects of partial discharges and their effects on materials," *1993 International Conference on Partial Discharge*, 1993, pp. 11-14.

[12] C. Abadie, "On-line non-intrusive partial discharge detection in aeronautical systems," PhD Thesis, University of Toulouse, 2017.

[13] A. Rumi, J. G. Marinelli, A. Cavallini and P. Seri, "Can corona resistant wires ensure reliability in aerospace machine insulation?," *2022 IEEE Electrical Insulation Conference (EIC)*, Knoxville, TN, USA, 2022, pp. 309-312.

[14] G. C. Montanari and P. Seri, "About the definition of PDIV and RPDIV in designing insulation systems for rotating machines controlled by inverters," *2018 IEEE Electrical Insulation Conference (EIC)*, 2018, pp. 554-557.

[15] A. Rumi, L. Lusuardi, A. Cavallini, M. Pastura, D. Barater and S. Nuzzo, "Partial discharges in electrical machines for the more electrical aircraft. Part III: preventing partial discharges," *IEEE Access*, vol. 9, pp. 30113-30123, 2021.
[16] L. Lusuardi, A. Cavallini, A. Caprara, F. Bardelli and A. Cattazzo, "The impact of test voltage waveform in determining the repetitive partial discharge inception voltage of Type I turn/turn insulation used in inverter-fed induction motors," *2018 IEEE Electrical Insulation Conference (EIC)*, San Antonio, TX, USA, 2018, pp. 478-481.
[17] H. Naderiallaf, P. Giangrande, and M. Galea, "Characterization of PDIV, PDEV, and RPDIV in insulated wires under unipolar repetitive square wave excitations for inverter-fed motors," *IEEE Access*, vol. 11, pp. 51047-51063, 2023.
[18] A. Contin, A. Cavallini, G. C. Montanari, G. Pasini, and F. Puletti, "Digital detection and fuzzy classification of partial discharge signals," *IEEE Trans. Dielectr. Electr. Insul.*, vol. 9, no. 3, pp. 335–348, Jun. 2002.
[19] IEEE Std 286-2000, *IEEE recommended practice for measurement of power factor tip-up of electric machinery stator coil insulation*, 2001.
[20] P. Wang, A. Cavallini, G. C. Montanari and G. Wu, "Effect of rise time on PD pulse features under repetitive square wave voltages," *IEEE Trans. Dielec. Elec. Insul.*, vol. 20, no. 1, pp. 245-254, February 2013.
[21] H. Naderiallaf, P. Giangrande and M. Galea, "Glass fibre insulated wire assessment under partial discharges activity via dielectric dissipation factor measurements," *2022 9th International Conference on Condition Monitoring and Diagnosis (CMD)*, Kitakyushu, Japan, 2022, pp. 98-102.
[22] M. Farahani, H. Borsi and E. Gockenbach, "Study of capacitance and dissipation factor tip-up to evaluate the condition of insulating systems for high voltage rotating machines," *Electrical Engineering*, vol. 89, no. 4, pp. 263-270, 2007.
[23] P. Seri, H. Naderiallaf and G. C. Montanari, "Modelling of supply voltage frequency effect on partial discharge repetition rate and charge amplitude from AC to DC at room temperature," *IEEE Trans. Dielec. Elec. Insul.*, vol. 27, no. 3, pp. 764-772, June 2020.
[24] A. Cavallini, G. C. Montanari and M. Tozzi, "Electrical aging of inverter-fed wire-wound induction motors: from quality control to end of life," *2010 IEEE International Symposium on Electrical Insulation*, San Diego, CA, USA, 2010, pp. 1-4.
[25] L. Fornasari, A. Caprara and G. C. Montanari, "Partial discharge measurements in electrical machines controlled by variable speed drives: from design validation to permanent PD monitoring," *9th IEEE International Symposium on Diagnostics for Electric Machines, Power Electronics and Drives (SDEMPED)*, pp. 384-390, Aug. 2013.
[26] H. Naderiallaf, P. Seri, and G. C. Montanari, "Effect of voltage slew rate on partial discharge phenomenology during voltage transient in HVDC insulation: the case of polymeric cables," *IEEE Trans. Dielectr. Electr. Insul.*, vol. 29, no. 1, pp. 215-222, Feb. 2022.
[27] H. Naderiallaf, R. Ghosh, P. Seri and G. C. Montanari, "HVDC insulation systems: effect of voltage polarity inversion slew rate on partial discharge phenomenology and harmfulness," *22nd International Symposium on High Voltage Engineering (ISH 2021)*, 2021, pp. 7-12.